Microstructures and Thermal Behaviour of $Ti_{31.75}V_{18.25}Pt_{50}$ and $Ti_{25}V_{25}Pt_{50}$ Potential Shape Memory Alloys

***[1]TM Motsai, *[2]ME Makhatha, [1]ST Camagu, [1]C Machio, [1]P Daswa, [1]PM Radingoana and [1,3]GT Motsi**

[1] Advanced Materials Engineering, Manufacturing Cluster, Council for Scientific and Industrial Research, P.O. Box 395, Pretoria, 0001, South Africa
[2] Department of Metallurgy, School of Mining, Metallurgy and Chemical Engineering, University of Johannesburg, Doornfontein Campus, Johannesburg,2028, South Africa
[3] University of Pretoria, Department of Materials Science and Metallurgical Engineering. Private bag X20, Hatfield 0002, South Africa

Abstract

The binary $Ti_{50}Pt_{50}$ alloy exhibits high transformation temperatures (1050°C) and has gained a great deal of attention due to its potential for high temperature applications in the automotive and aerospace industries. However, this binary system has negligible shape memory effect. Shape memory effect is the property of a material to recover to its initial shape following heating while retaining residual deformations throughout an inelastic loading/unloading cycle. Improved shape memory properties could be achieved by ternary alloying $Ti_{50}Pt_{50}$. A study reported on partial substitution of Ti with 6.25 and 12.5 at. % V in the equi-atomic TiPt resulted in increased austenite and martensitic transformation temperature. This study is a follow-up to investigate the impact of higher V contents (18.25 and 25 at. %) on microstructures and the thermal behaviour of the alloys. Samples were prepared by arc melting of blended powders, and characterised for microstructures, thermal behaviour and hardness. The as-cast microstructure of $Ti_{31.75}V_{18.25}Pt_{50}$ revealed a matrix of a single phase (Ti, V) Pt and second phases comprising TiO and (Ti_2O) + Pt, while that of $Ti_{25}V_{25}Pt_{50}$ showed a matrix of (Ti,V) Pt with TiO and Ti_2O. Solution heat-treated $Ti_{31.75}V_{18.25}Pt_{50}$ showed a matrix of the single phase (Ti, V) Pt with second phases of (Ti, V) Pt, while $Ti_{25}V_{25}Pt_{50}$ showed a matrix of (Ti, V) Pt with second phases of (Ti, V) Pt, TiO, TiO_2 and Ti_2O. Increasing vanadium from 18.25 to 25 at. % led to a decrease in transformation temperature in both the as-cast and solution heat-treated conditions. The transformation temperature increased after solution heat treatment. The enthalpy change during transformation (ΔH) decreased with higher vanadium content. Hardness values increased with vanadium content increase in both as-cast and heat-treated conditions.

Keywords: TiPt, vanadium, shape memory alloys, martensitic transformation temperature

Introduction

Shape memory alloys (SMAs) are used in a variety of commercial applications owing to their unique shape memory effect (SME) and superelastic behaviour. Additional research, particularly in the area of high-temperature alloys, is expected to lead to even more widespread implementation of these multifunctional materials (Karakoc *et al.*, 2022). SME describes a material's capacity to hold onto residual deformations throughout an inelastic loading/unloading cycle while reverting to its original shape when heated (Sattari *et al.*, 2022). The mechanism behind SME is based on a phase transformation between austenite and martensite phases (Shirani and Kadkhodaei, 2015). The quantity of shape memory is primarily influenced by the amount of martensite in the alloy and the degree to which martensite is transformed into austenite (Sathish, Mallik and Raju, 2014). The martensitic change of austenite to martensite on cooling (through the martensite start and finish temperatures) and the reverse transformation on heating are both necessary for shape memory effect (through the austenite start and finish temperatures) (Frenzel *et al.*, 2010). Nickel-titanium alloys (NiTi) are the most widely used SMAs, however their operating temperature of ~100˚C excludes high-temperature applications (Karakoc *et al.*, 2022) (Chang *et al.*, 2021). The search for alloys with higher transformation temperatures has extensively focused on the titanium-platinum (TiPt) alloys. The binary equi-atomic TiPt system exhibits transformation temperatures above 1000˚C, much higher than observed for NiTi based shape memory alloys. A phase transformation from a high temperature austenitic B2 phase to a low temperature martensitic B19 phase occurs at a temperature of about 1050˚C. This makes it a potential material for application as a high temperature SMA (HTSMA) (Daswa, Chikosha and Siyasiya, 2021). However, TiPt based alloys show very low shape memory effect (Wadood *et al.*, 2013).

The poor shape memory properties of binary TiPt alloys are due to the low critical stress for slip deformation compared to the stress required for martensitic transformation. Application as HTSMAs therefore requires that this critical stress for slip deformation at high temperature be enhanced (Wadood *et al.*, 2013). These aforementioned properties can be improved through ternary alloying (Yamabe-Mitarai *et al.*, 2012), (Yamabe-Mitarai *et al.*, 2013), (Wadood and Yamabe-Mitarai, 2014), (Yamabe-Mitarai *et al.*, 2015), (Yamabe-Mitarai *et.al.* 2017). For example, the partial substitution of Pt with Ru and Co can improve mechanical and functional properties, however they decrease the martensitic transformation temperature (Figure 1) (Wadood and Yamabe-Mitarai, 2014). Note that the phase transformation process involves several temperatures. The temperatures at which the transformation begins and ends are A_S (austenite start) and A_f (austenite finish), and M_S (martensite start) and M_f (martensite finish), respectively, when the material is heated and cooled (Kneissl *et al.*, 2008). A similar response was obtained when Ti was partially substituted with Zr, where the phase transformation

temperatures, A_f and M_f, of 1066°C and 1012 °C of Ti–50Pt decreased to 804 °C and 590 °C with Zr additions respectively (Yamabe-Mitarai *et al.* 2017). On the other hand, partially replacing Pt with Ir, simultaneously improved the mechanical and functional properties and increased the martensitic transformation temperature. The A_f increased with increasing Ir content from 1058 °C in Ti-50 at. % Pt to 1218 °C in Ti-12.5Pt-37.5Ir. The Ti-25Pt-25Ir alloy resulted in the highest shape recovery ratio of 57 % after deformation at 850°C followed by heating to above A_f (Yamabe-Mitarai *et al.*, 2012). Substitutional elements with the largest difference in atomic radius from Pt were found to be more efficient in increasing mechanical properties. (Yamabe-Mitarai *et al.*, 2015). A new alloying element that has recently attracted attention is vanadium. Vanadium has no preference for Ti or Pt sites, according to TiPt-X ternary computational simulations (Bozzolo, Mosca and del Grosso, 2008), and would therefore occupy sites on either sub-lattice with equal probability (Chikosha *et al.*, 2018). An initial study was conducted, where partial substitution of Ti with 6.25 and 12.5at.% V was investigated and resulted in improved transformation temperature and functional properties of the SMA (Daswa *et al.*, 2021). This current study is a follow-on study, to investigate the effect of higher V contents (V>12.5at%) on the phase transformations of Ti50Pt50 alloy. Alloys with vanadium contents of 18.25 and 25 at. %, replacing for Ti, have been prepared to investigate the effect of higher V contents on the evolution of microstructure during heat treatment, the thermal behaviour and hardness.

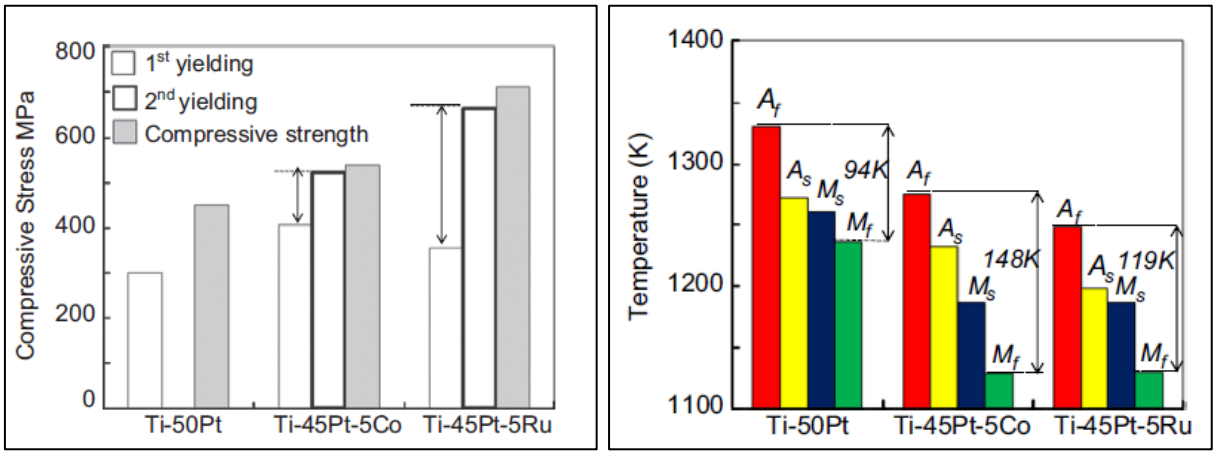

Figure 1. A graphs illustrating the yield stress and high temperature compressive strength for 20% applied strain at 50 K below M_f and phase transformation temperatures of Ti-50Pt, Ti-45Pt-5Co and Ti-45Pt-5Ru (Wadood and Yamabe-Mitarai, 2014).

Experimental procedure

In order to produce homogeneous blends with nominal compositions, high purity Ti(99.9%), Pt(99.9%), and V(99.5%) powders were measured into desired quantities. TLS Technik GmbH & Co., Germany supplied the elemental Ti powder, while LGC Industrial Analytical (Pty) Ltd. in South Africa supplied the

elements Pt and V powders. The powders, of mass 5 g, were compacted in a die of size 18 mm using An Enerpac VLP 100 tonne press to form buttons for arc melting. To improve chemical homogeneity, the buttons were turned over six times during melting. To minimise oxidation, melting was done under argon. In addition, titanium buttons were loaded into the furnace to act as oxygen getters. Following casting, the alloy ingots were solution heat-treated for 72 hours at 1250°C in a Carbolite tube furnace under argon gas followed by quenching in ice water.

The homogeneity, chemical composition, and microstructure of the alloys were analysed using a scanning electron microscope (JEOL JSM-6510) in backscatter mode with energy dispersive spectrometer (EDS), for semi-quantitative composition analysis. Differential scanning calorimetry (Netzsch STA 449F3 Jupiter calorimeter) with simultaneous thermal analyser (STA) was used to measure the phase transformation temperatures and thermal stability (five cycles per sample). The thermal stability investigations were done at a ramp rate of 10°C/min under a 10 ml/min argon gas flow, repeated five times. A macro Vickers hardness tester (FV-700) was used to conduct hardness tests with a weight of 2 kg and dwell duration of 10 seconds. Vickers hardness (VHN) was determined from the average of five readings per sample.

Results and discussion

Microstructure

Figure 2 shows the microstructure of $Ti_{31.75}V_{18.25}Pt_{50}$ in the as-cast [Figures 2 (a & b)] and solution heat-treated [Figures 2 (c & d)] conditions. The as-cast sample in Figure 2 (a) shows inhomogeneity where dark and light grey regions comprising of (Ti, V) Pt are observed. Additionally, dendrites of TiO were observed, Figure 2 (b), indicating the occurrence of some oxidation during the arc-melting process. This could be due to partitioning of alloying elements during solidification, resulting in the formation of dendrites and inhomogeneity (Ramaiah *et al.*, 2013).

Solution heat treatment did not eliminate the inhomogeneity, observed in the as-cast state Figure 2 (c & d). It is possible that the persistent inhomogeneity was due to insufficient solution heat treatment time. A similar solution heat treatment cycle had generated homogeneous microstructures in $Ti_{43.75}V_{6.25}Pt_{50}$ and $Ti_{37.5}V_{12.5}Pt_{50}$ (Daswa, Siyasiya and Chikosha, 2020). The sample consisted of (Ti, V) Pt, the matrix, with a dispersion of dark spots of probably TiO, after solution heat treatment. The (Ti,V)Pt phase had two grey level contrasts, due to different Pt contents (Table 1).

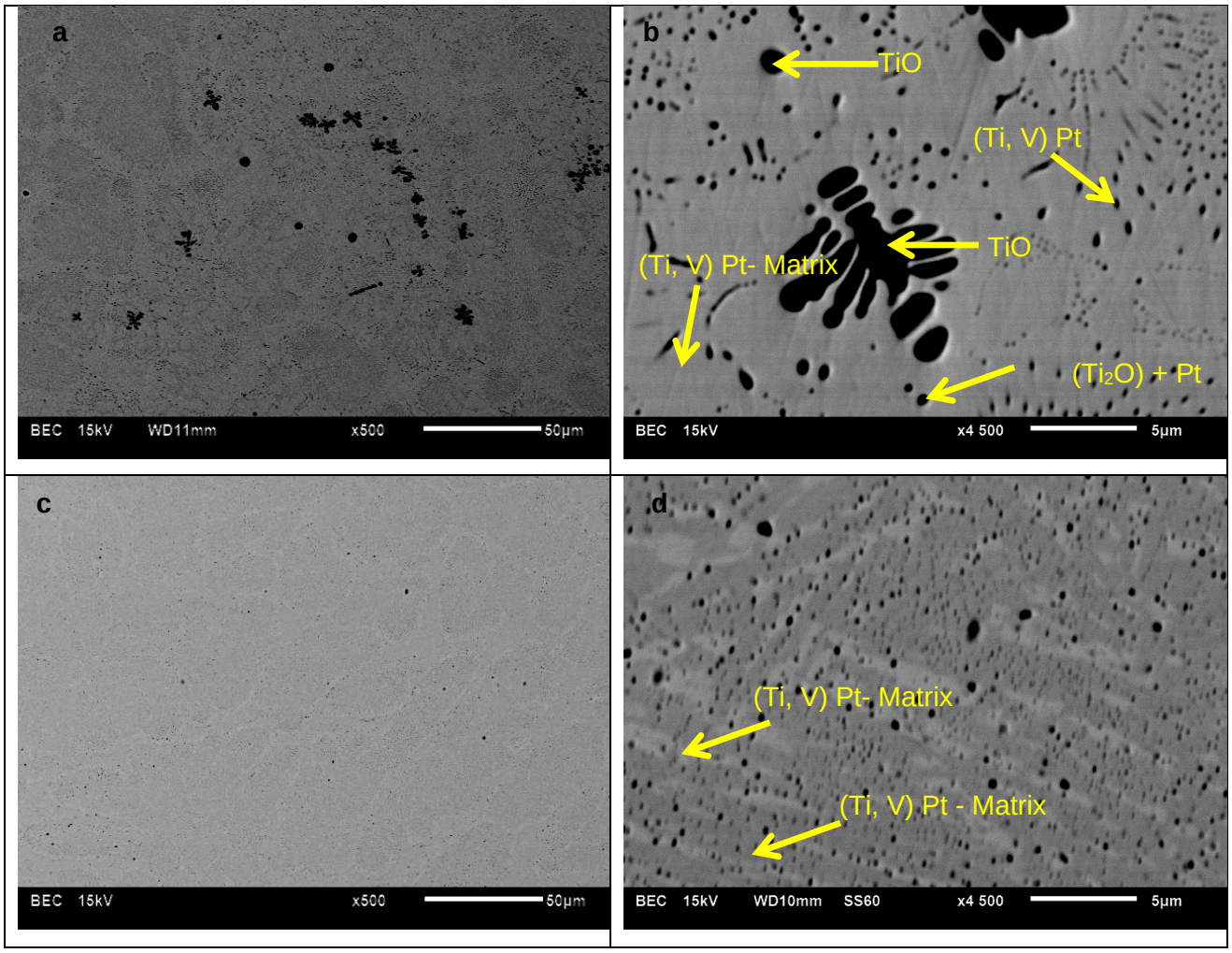

Figure 2. SEM backscattered micrographs of as-cast and solution heat-treated $Ti_{31.75}V_{18.25}Pt_{50}$ alloys, low magnification (a & c) and high magnification (c & d) respectively.

EDS analysis of the compositions in the as-cast and solution heat-treated conditions of alloy $Ti_{31.75}V_{18.25}Pt_{50}$ revealed Pt contents of 49 and 53 at. %, respectively (Table I). The analysis also indicated that V had gone into solution, to form (Ti,V)Pt, equivalent to TiPt, the phase that transforms during heating and cooling. Above the transformation temperature of titanium, titanium and vanadium form a solid solution (Duwez, 1952). The (Ti, V) Pt had varying V contents both in the as-cast condition and in the heat-treated condition. While the variation in composition could have been caused by overlap of areas being analysed due to electron beam spreading out, in this paper the existence of different grey level contrast does support the changing compositions. Generally, however, the overall compositions in both the as-cast and solution heat-treated conditions were within the single phase TiPt region of the TiPt phase diagram where the Pt content ranges between 46 and 54 at.%.

Table I. Characteristic SEM EDS analysis of $Ti_{31.75}V_{18.25}Pt_{50}$ in both the as-cast and solution heat-treated conditions

Phase	O (at. %)	Ti (at. %)	V (at. %)	Pt (at. %)
		As-Cast		
Overall	**-**	**35**	**16**	**49**
TiO	53	45	2	-
(Ti, V) PT	-	35	13	42
(Ti, V) Pt	-	22	21	57
		Solution treated		
Overall	**-**	**30**	**17**	**53**
(Ti, V) Pt	-	29	19	52
(Ti, V) Pt	-	36	13	51

The microstructures of the $Ti_{25}V_{25}Pt_{50}$ were similar to those of $Ti_{31.75}V_{18.25}Pt_{50}$ in that as-cast microstructures consisted of a (Ti, V) Pt matrix with dendritic areas of TiO and Ti_2O [Figure 3 (a & b)]. Solution heat treatment did not result in full elimination of dendrites as shown in Figure 3 (c & d). Table II shows the characteristic EDS results of the $Ti_{25}V_{25}Pt_{50}$ alloy in the as-cast and solution heat-treated conditions. The overall Pt contents were found to be 49 and 47 at. % respectively. The transforming phases (Ti, V) Pt had V contents of 16 at. % in the as-cast condition and 22 at. % in the heat-treated condition. The overall compositions in both conditions were within the single phase TiPt region where the Pt content ranges between 46 and 54 at.%.

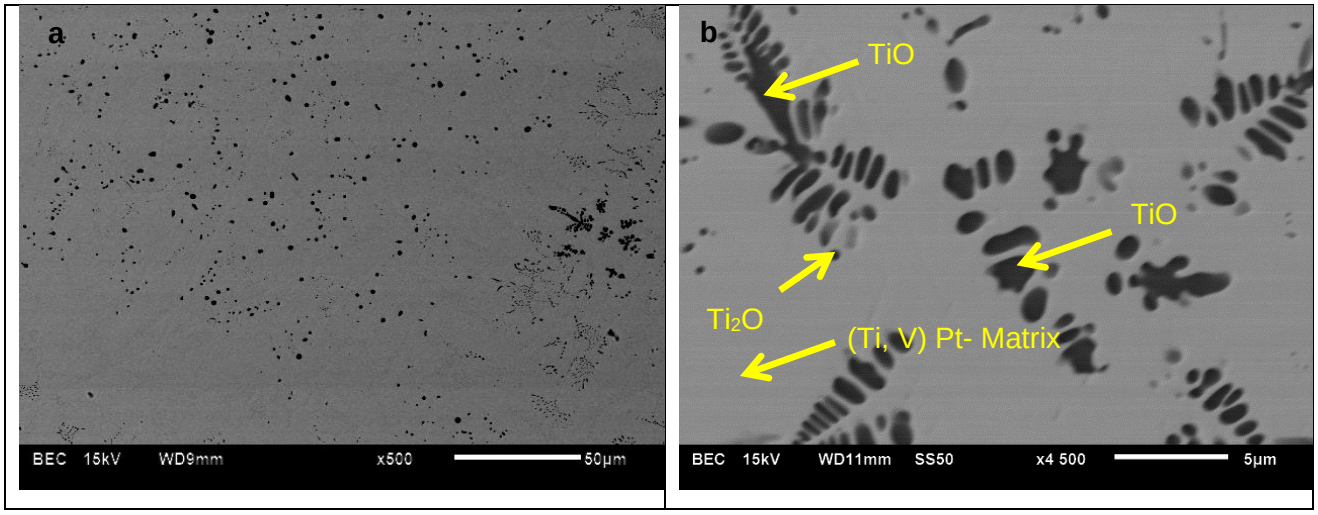

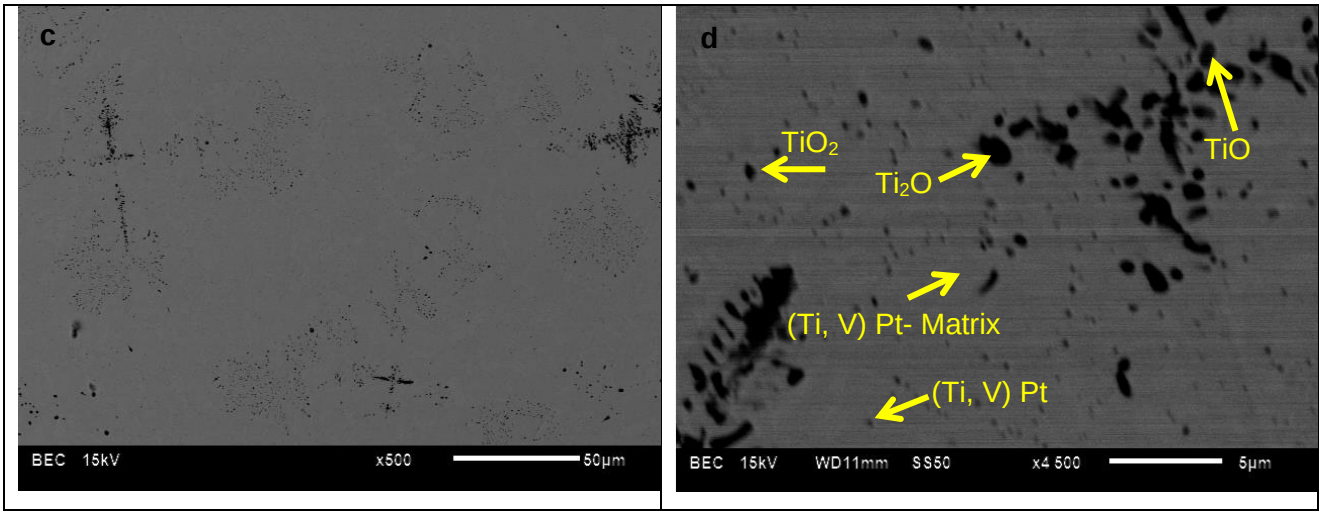

Figure 3: SEM backscattered micrographs of as-cast and solution heat-treated $Ti_{25}V_{25}Pt_{50}$ alloys, low magnification (a & c) and high magnification (c & d) respectively.

Table II. Characteristic SEM EDS results of $Ti_{25}V_{25}Pt_{50}$ in both the as-cast and solution heat-treated conditions

Phase	O (at. %)	Ti (at. %)	V (at. %)	Pt (at. %)
		As-Cast		
Overall	**-**	**35**	**16**	**49**
Ti_2O	32	62	-	6
TiO	48	34	5	13
(Ti, V) Pt	-	30	14	56
		Solution heat treated		
Overall	**-**	**31**	**22**	**47**
TiO	47	46	5	2
(Ti, V) Pt	-	19	26	55

Phase transformation temperatures

Figure 4 presents the fourth cycle thermal behaviour of the as-cast and solution heat-treated, $Ti_{31.75}V_{18.25}Pt_{50}$ and $Ti_{25}V_{25}Pt_{50}$ alloys. The fourth cycle was used because all the alloys showed peaks both on heating and cooling on the fourth and fifth cycles. The solid lines show the heating cycle while the dashed lines show the cooling cycle. The respective transformation temperatures, hysteresis, and enthalpy of the alloys of the present study, in comparison to solution heat-treated $Ti_{50}Pt_{50}$ (Daswa *et al.,* 2021), $Ti_{43.75}V_{6.25}Pt_{50}$ (Daswa *et al.,* 2021), $Ti_{37.5}V_{12.5}Pt_{50}$ (Daswa *et al.,* 2021) are shown in Table III. In the as-cast condition, the M_s transformation temperatures decrease from 1361°C to 1171°C with

increasing V content, similar behaviour was observed with the solution heat-treated alloys. The decrease in transformation temperature observed in the two processing conditions, with the increase in vanadium content, could be attributed to inhomogeneous microstructures as observed in $Ti_{25}V_{25}Pt_{50}$ alloy. The solution heat treatment condition generally increases the M_s transformation temperatures to values of 1471°C and 1417°C , for both 18.25 and 25 at.% V alloys, respectively. In comparison to literature, for solution heat-treated alloys, when V content was increased from 6.25 at. % (Daswa, Siyasiya and Chikosha, 2020) to 25 at.% (present study) the A_s and M_s transformation temperature gradually increases. The A_s and M_s of the $Ti_{50}Pt_{50}$ alloy increased from 1031°C and 1014°C to 1070°C and 1112 °C with 6.25 at. % V and 1175°C and 1292°C with 12.5 at.% V additions respectively (Daswa, Siyasiya and Chikosha, 2020).

The enthalpy change during transformation, ΔH, given by the area under the curve, for both alloys in both conditions are small and decrease with the increase in vanadium; for example, ΔH of the forward transformation for the as-cast 18.25 at.% V, 25 at. % V, solution heat-treated 18.25 at. % V and 25 at. % V alloys are 10.68, 0.30, 1.26 and 0.20 (J/g) respectively. Similar observations were made in literature (Daswa, Siyasiya and Chikosha, 2020) . There is a decrease in the latent heat of formation (ΔH) when vanadium is increased from 18.25 to 25 at. %. It could be that the addition of Vanadium contributes to the stabilisation of the B2 phase structure, which prevents the martensite phase from forming, or that the vanadium reduces the geometrical differences in the crystal structures of the B2 and the martensite phases, as occurs in Ni-Ti alloys (Frenzel *et al.*, 2015).

The increase in vanadium content resulted in a decrease of the thermal hysteresis (ΔT) from 63 to 26 and 20 to 4 in $Ti_{31.75}V_{18.25}Pt_{50}$ and $Ti_{25}V_{25}Pt_{50}$ respectively. The decrease in the thermal hysteresis with solution heat treatment when vanadium was increased from 6.25 to 12.5 at.% was also observed (Daswa *et al.*, 2021). A similar reduction in hysteresis in Ni-Ti alloys has been attributed to diminishing differences in the geometrical lattices of the B2 and the martensite phase (Frenzel et al., 2015). Further work will be performed to model the evolution of the lattices of the TiPt with increasing V contents.

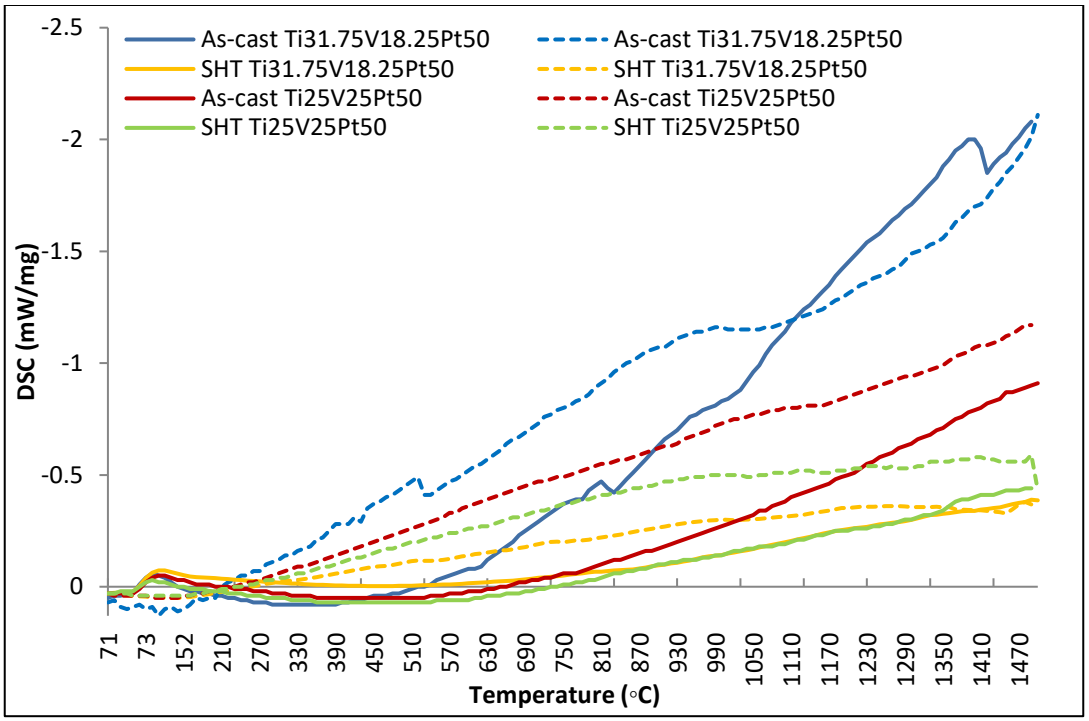

Figure 4. Fourth DSC thermal cycles of $Ti_{31.75}V_{18.25}Pt_{50}$ and $Ti_{25}V_{25}Pt_{50}$ in the as-cast and solution heat treated (1250 ºC for 72 hours).

Table III. Transformation temperatures, hysteresis and enthalpy of (Ti,V)Pt during the fourth DSC heating and cooling thermal cycles in the as-cast and solution heat-treated conditions

	Alloy	A_s (°C)	A_f (°C)	M_s (°C)	M_f (°C)	ΔT(°C)	ΔH (J/g) Forward	ΔH (J/g) Reverse
As-Cast	$Ti_{50}Pt_{50}$	1031	1076	1015	986	61	26.0	-23.5
	$Ti_{43.75}V_{6.25}Pt_{50}$	1077	1208	1095	1041	113	16.4	-22.2
	$Ti_{37.5}V_{12.5}Pt_{50}$	1171	1386	1296	1228	90	12.6	-29.2
	$Ti_{31.75}V_{18.25}Pt_{50}$	1394	1424	1361	1344	63	10.7	0.40
	$Ti_{25}V_{25}Pt_{50}$	1185	1191	1171	1166	20	0.30	0.25
SHT: (1250 °C, 72 hrs.)	$Ti_{50}Pt_{50}$	1031	1074	1014	981	60	18.6	-16.9
	$Ti_{43.75}V_{6.25}Pt_{50}$	1070	1215	1112	1032	103	17.9	-27.8
	$Ti_{37.5}V_{12.5}Pt_{50}$	1175	1380	1292	1193	88	12.8	-25.4
	$Ti_{31.75}V_{18.25}Pt_{50}$	1480	1497	1471	1426	26	1.26	-3.95
	$Ti_{25}V_{25}Pt_{50}$	1407	1421	1417	1399	4	0.20	0.063

Hardness

Figure 5 shows the hardness results of the two TiVPt alloys in the as-cast and solution heat-treated conditions. The hardness of as-cast was irregular with an increase, whereas after solution heat treatment, a linear increase was observed with an increase in vanadium concentration. The hardness of as-cast $Ti_{50}Pt_{50}$ alloy increased to 583HV with addition of 18.25 at.% V, then decreased to 506HV with 25 at.% V addition. Solid solution strengthening due to the dissolution of V in the Ti-Pt phase and presence of second phases can explain the high hardness values (Biggs *et al.*, 2001). The decrease

in hardness as vanadium content could be due to finer TiO dendrites in the 25 at. %V alloy as compared to the coarser dendrites in the 18.25 at. % V alloy.

The opposite is observed in the solution heat-treated state where hardness gradually increased to 591 HV with the addition of 25 at.% V, similar results were obtained in literature where hardness increased from 522 and 565 HV in the as-cast state of $Ti_{50}Pt_{43.75}V_{6.25}$ and $Ti_{50}Pt_{37.5}V_{12.5}$ respectively to 547 and 669 HV after heat treatment (Daswa *et al.*, 2021). This could be attributed to high V contents in solid solution with Ti-Pt phase resulting in improved homogenisation and also the presence of second phases (Biggs *et al.*, 2001). In general, the current results indicate that ternary alloying of $Ti_{50}P_{50}$ alloy with vanadium and solution heat treatment – both contribute to the increase in hardness.

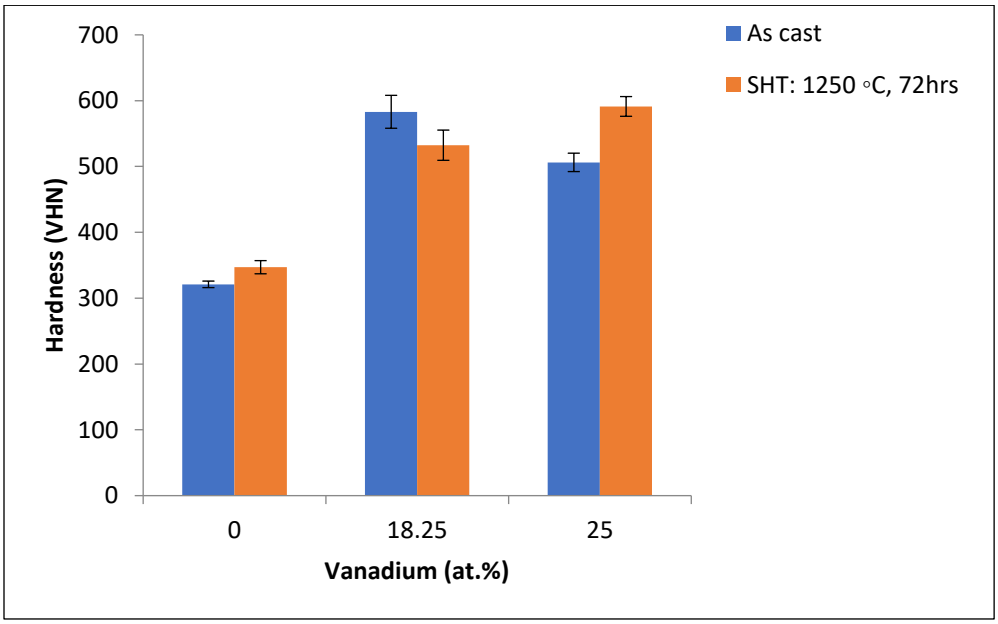

Figure 5. Macro Vickers hardness of TiVPt alloys as a function of V content in the as-cast and solution heat-treated (SHT) conditions.

Conclusions

The following conclusions were drawn from the study:

- In both the as-cast and solution heat-treated conditions, the overall compositions of both alloys were within the single phase TiPt region, with Pt content ranging from 46 to 54 at.%.
- TiO based phases were observed in both alloys.

- Increasing vanadium from 18.25 to 25 at. % decreases the transformation temperature in both the as-cast and solution heat-treated conditions.
- Solution heat treatment increases the transformation temperature.
- The increase in vanadium decreases the latent heats of formations.
- The improvement in hardness is aided by ternary alloying of $Ti_{50}Pt_{50}$ with vanadium and solution heat treatment.

Acknowledgements

The funding support for this work by the Titanium Centre of Competence (TiCoC), the Council for Scientific and Industrial Research and the University of Johannesburg is gratefully acknowledged.

References

Biggs, T., Cortie, M. B., Witcomb, M. J., and Cornish, L. A. (2001) 'Martensitic transformations, microstructure, and mechanical workability of TiPt', *Metallurgical and Materials Transactions A: Physical Metallurgy and Materials Science*, 32(8), pp. 1881–1886. doi: 10.1007/s11661-001-0001-5.

Bozzolo, G., Mosca, H. O. and del Grosso, M. F. (2008) 'Energy of formation, lattice parameter and bulk modulus of (Ni,X)Ti alloys with X = Fe, Pd, Pt, Au, Al, Cu, Zr, Hf', *Intermetallics*, 16(5), pp. 668–675. doi: 10.1016/J.INTERMET.2008.02.003.

Chang, S. H., Kao, W. P., Hsiao, K. Y., Yeh, J. W., Lu, Ming, Y., and Tsai, C. W. (2021) 'High-temperature shape memory properties of Cu15Ni35Ti25Hf12.5Zr12.5 high-entropy alloy', *Journal of Materials Research and Technology*, 14, pp. 1235–1242. doi: 10.1016/j.jmrt.2021.07.008.

Chikosha, S., Mahlatji, M. L., Modiba, R. and Chikwanda, H.K. (2018) 'The effect of vanadium on structure and martensitic transformation temperature of TiPt alloy', *IOP Conference Series: Materials Science and Engineering*, 430(1). doi: 10.1088/1757-899X/430/1/012022.

Daswa, P., Chikosha, S. and Siyasiya, C. W. (2021) 'Shape memory properties and transformation temperature of Ti50-XVXPt50 alloy', *Intermetallics*, 133(March), p. 107154. doi: 10.1016/j.intermet.2021.107154.

Daswa, P., Siyasiya, C. W. and Chikosha, S. (2020) 'The effect of ternary alloying on the shape memory properties of titanium-platinum alloys', (August). Available at: http://hdl.handle.net/2263/79641.

Duwez, P. (1952) 'Partial Titanium-Vanadium Phase Diagram', (June), pp. 627–630.

Frenzel, J. *et al.* (2010) ‘Influence of Ni on martensitic phase transformations in NiTi shape memory alloys’, *Acta Materialia*, 58(9), pp. 3444–3458. doi: 10.1016/j.actamat.2010.02.019.

Frenzel, J., George, E. P., Dlouhy, A., Somsen, C. H., Wagner, M. F.X., and Eggeler, G. (2015) ‘On the effect of alloy composition on martensite start temperatures and latent heats in Ni-Ti-based shape memory alloys’, *Acta Materialia*, pp. 213–231. doi: 10.1016/j.actamat.2015.02.029.

Karakoc, O., Atli, K. C., Benafan, O., Noebe, R. D., and Karaman, I. (2022) ‘Actuation fatigue performance of NiTiZr and comparison to NiTiHf high temperature shape memory alloys’, *Materials Science and Engineering A*, 829(October 2021), p. 142154. doi: 10.1016/j.msea.2021.142154.

Kneissl, A., Unterweger, E., Bruncko, M., Mehrabi, K., Lojen, G., and Scherngell, H. (2008) ‘Microstructure and properties of Niti and Cualni shape memory alloys’, *Metalurgija*, 14(2), pp. 89–100.

Ramaiah, K. V., Saikrishna, C. N., Sujata, M., and Bhaumik, S. K. (2013) ‘Ni30 Ti50 Pt20 High Temperature Shape Memory Alloy (HTSMA) Wires : Processing Related Issues’, *Journal of ISSS*, 2(2), pp. 1–9.

Sathish, S., Mallik, U. S. and Raju, T. N. (2014) ‘Microstructure and Shape Memory Effect of Cu-Zn-Ni Shape Memory Alloys’, *Journal of Minerals and Materials Characterization and Engineering*, 02(02), pp. 71–77. doi: 10.4236/jmmce.2014.22011.

Sattari, M., Kadkhodaei, M., Akbarzadeh, S., Gholami, R., and Beheshti, A. (2022) ‘Wear in superelastic shape memory alloys: A thermomechanical analysis’, *Wear*, 488–489(October 2021), p. 204139. doi: 10.1016/j.wear.2021.204139.

Shirani, M. and Kadkhodaei, M. (2015) ‘One dimensional constitutive model with transformation surfaces for phase transition in shape memory alloys considering the effect of loading history’, *International Journal of Solids and Structures*. doi: 10.1016/j.ijsolstr.2015.11.019.

Wadood, A., Takahashi, M., Takahashi, S., Hosoda, H., and Yamabe-Mitarai, Y. (2013) ‘High-temperature mechanical and shape memory properties of TiPt-Zr and TiPt-Ru alloys’, *Materials Science and Engineering A*, 564, pp. 34–41. doi: 10.1016/j.msea.2012.11.069.

Wadood, A. and Yamabe-Mitarai, Y. (2014) ‘TiPt-Co and TiPt-Ru high temperature shape memory alloys’, *Materials Science and Engineering A*, 601, pp. 106–110. doi: 10.1016/j.msea.2014.02.029.

Yamabe-Mitarai, Y., Hara, T., Miura, S., and Hosoda,. (2012) ‘Phase transformation and shape memory effect of Ti(Pt, Ir)’, *Metallurgical and Materials Transactions A: Physical Metallurgy and*

Materials Science, 43(8), pp. 2901–2911. doi: 10.1007/s11661-011-0954-y.

Yamabe-Mitarai, Y., Hara, T., Kitashima, T., Miura, S., and Hosoda, H. (2013) 'Composition dependence of phase transformation behavior and shape memory effect of Ti(Pt, Ir)', *Journal of Alloys and Compounds*, 577(SUPPL. 1), pp. S399–S403. doi: 10.1016/j.jallcom.2012.02.136.

Yamabe-Mitarai, Y., Arockiakumar, R., Wadood, A., Suresh, K.S., Kitashima, T., Hara, T., Shimojo, M., Tasaki, W., Takahashi, M., Takahashi, S., and Hosoda, H. (2015) 'Ti(Pt, Pd, Au) based High Temperature Shape Memory Alloys', *Materials Today: Proceedings*, 2, pp. S517–S522. doi: 10.1016/j.matpr.2015.07.338.

Yamabe-Mitarai, Y., Takebe, W. and Shimojo, M. (2017) 'Phase Transformation and Shape Memory Effect of Ti–Pd–Pt–Zr High-Temperature Shape Memory Alloys', *Shape Memory and Superelasticity*, 3(4), pp. 381–391. doi: 10.1007/s40830-017-0131-2.